SUPPLEMENTARY APPENDIX

TAK1 is a pivotal therapeutic target for tumor progression and bone destruction in myeloma

Jumpei Teramachi,[1,2] Hirofumi Tenshin,[2,3] Masahiro Hiasa,[2,3] Asuka Oda,[2] Ariunzaya Bat-Erdene,[2,4] Takeshi Harada,[2] Shingen Nakamura,[2] Mohannad Ashtar,[2,3] So Shimizu,[2,3] Masami Iwasa,[2] Kimiko Sogabe,[2] Masahiro Oura,[2] Shiro Fujii,[2] Kumiko Kagawa,[2] Hirokazu Miki,[5] Itsuro Endo,[6] Tatsuji Haneji,[1] Toshio Matsumoto[7] and Masahiro Abe[2]

[1]Department of Histology and Oral Histology, Tokushima University Graduate School, Tokushima, Japan; [2]Department of Hematology, Endocrinology and Metabolism, Tokushima University Graduate School, Tokushima, Japan; [3]Department of Orthodontics and Dentofacial Orthopedics, Tokushima University Graduate School, Tokushima, Japan; [4]Department of Immunology and Laboratory Medicines, School of Biomedicine, Mongolian National University of Medical Sciences, Ulaanbaatar, Mongolia; [5]Division of Transfusion Medicine and Cell Therapy, Tokushima University Hospital, Tokushima, Japan; [6]Department of Chronomedicine, Institute of Biomedical Sciences, Tokushima University Graduate School, Tokushima, Japan and [7]Fujii Memorial Institute of Medical Sciences, Tokushima University, Tokushima, Japan

 doi:10.3324/haematol.2019.234476

Received: August 7, 2019.

Accepted: April 2, 2020.

Pre-published: April 9, 2020.

Correspondence: *JUMPEI TERAMACHI* - jumptera@okayama-u.ac.jp

MASAHIRO ABE - masabe@tokushima-u.ac.jp

SUPPLEMENTARY INFORMATION

SUPPLEMENTAL MATERIALS AND EXPERIMENTAL PROCEDURES

Reagents

The following reagents were purchased from the indicated manufacturers: Antibodies against phosphorylated TAK1 and p84 from Abcam (Cambridge, MA); antibodies against phosphorylated p38MAPK, p38 MAPK, phosphorylated 4E-BP1, 4E-BP1, p65, caspase 8, cleaved caspase 8, caspase 9, cleaved caspase 9, caspase 3, cleaved caspase 3, c-fos, MYC, phosphorylated ERK, ERK, phosphorylated IκBα, IκBα, IRF4, Osterix, PIM2, phosphorylated Smad1/5, phosphorylated Smad2, Smad2, phosphorylated-Smad3, Smad3, Smad5, Smad6, Sp1, phosphorylated STAT3, STAT3, TAK1, and GAPDH from Cell Signaling (Danvers, MA); antibodies against cathepsin K, Mcl-1, $NFATc_1$ (7A6), VCAM-1, α_4 integrin, and β_1 integrin, and normal mouse IgG from Santa Cruz Biotechnology (Santa Cruz, CA); anti-β-actin antibody Sigma-Aldrich (St. Louis, MO); LL-Z1640-2 (LLZ) (5Z-7-oxozeaenol) from Enzo Biochem (Farmingdale, NY); SMI-16a from Calbiochem (Darmstadt, Germany); recombinant mouse RANKL and M-CSF from PeproTech EC (London, UK); and recombinant human BMP-2 from R&D Systems (Minneapolis, MN).

Cells and cell culture

Peripheral blood mononuclear cells (PBMCs) and bone marrow mononuclear cells were isolated from healthy volunteers or patients with MM as previously described.[1]

The human MM cell lines KMS-11, KMS-12-BM, MM.1S, OPM-2, RPMI8226, and U266-B1 were obtained from the American Type Culture Collection (ATCC, Rockville, MD); TSPC-1 was established in our laboratory.[2] The human MM cell lines INA-6 was kindly provided by Dr. Renate Burger (University of Kiel, Kiel, Germany). Cells were cultured in RPMI1640 medium (Sigma, Aldrich, MO) supplemented with 10% FBS (Life Technologies, Grand Island, NY), penicillin G at 50 μg/ml and streptomycin at 50 μg/ml. MM cells were purified from bone marrow mononuclear cells from patients with MM by positive selection using anti-CD138 microbeads and Miltenyi magnetic cell sorting system (Miltenyi Biotec, Auburn, CA), in accordance with the manufacturer's instructions. Collection and expansion of BMSCs was performed as described previously.[2,3] All procedures involving human samples from healthy donors and patients were performed with written informed consent in accordance with the Declaration of Helsinki and a protocol approved by the Institutional Review Board for human

protection at University of Tokushima (Permission number: 240).

***in vitro* osteoclastogenesis**

The mouse pre-osteoclastic cell line RAW264.7 cells were cultured in 96-well culture plates (750 cells per well) in α-MEM containing 10% FBS for 4 days in the presence of RANKL (25 ng/ml), as described previously.[4] The cells were stained for TRAP after culturing for 3 days, and TRAP-positive multinucleated cells (MNCs) were counted.

The formation of osteoclasts from mouse bone marrow cells was performed as described previously.[5,6] Primary mouse bone marrow cells were isolated from the tibiae or femurs of 5-week-old male C57BL/6J mice. The cells (10^6 cells per well in 24-well plates) were pretreated with RANKL (25 ng/ml) and M-CSF (10 ng/ml) for 1 day, and then RPMI8226, KMS11, U266-B1, or INA-6 cells at 10^3cells/well were co-cultured for 5 days in RPMI1640 plus 10% FBS. The cells were stained for TRAP after the 3-day cultivation, and TRAP-positive MNCs were counted.

For immunofluorescence staining were performed as described previously. [6]

RAW264.7 cells was cultured with RANK ligand (50 ng/ml) for 30 minutes on glass bottomed

dishes. The cells were fixed and permeabilized, and then subsequently probed with an anti-p65 antibody overnight, followed by an incubation with Alexa Fluor 594-conjugated anti-rabbit IgG secondary antibody. The nuclei were stained with Hoechst 33342 (Dojindo). Wide field-of-view fluorescence images were examined using a fluorescence microscope (BX50, Olympus, Tokyo, Japan).

Osteoblast differentiation

Mouse pre-osteoblastic cell line MC3T3-E1 cells were cultured in 24-well culture plates in an osteogenic medium, α-MEM containing 10% FBS, 25 nM BMP-2, 10 mM β-glycerophosphate, and 50 mg/ml ascorbic acid, as previously described.[7] The medium was replaced every 3 days. To analyze mineralized nodules, cells were fixed with 10% neutral-buffered formalin (Wako Pure Chemical, Osaka, Japan) and visualized using Alizarin red staining as described.[7]

VEGF ELISA assay

Human MM cell lines were cultured for 1 day. Concentrations of VEGF in their culture media were determined using an ELISA kit for human VEGF (R&D) in accordance with the

manufacturer's instructions.

Myeloma animal model and histological analyses

All animal experiments were conducted under the regulation and permission of the Animal Care and Use Committee of Tokushima University, Tokushima, Japan (toku-dobutsu 13094). MM mouse models were prepared by intra-tibial inoculation of mouse *luciferase*-transfected 5TGM1 MM cells (a gift from Dr Gregory R. Mundy [Vanderbilt Center for Bone Biology, Vanderbilt University, Nashville, TN, USA]) to ICR nu/nu mice (CLEA Japan) at 4–6 weeks old as described previously.[5,7] Mice were treated with LLZ1640-2 intraperitoneally at 20 mg/kg or saline every other day for 2 weeks after confirming MM cell growth on day 5. Mouse sera were collected on day 6, 12, and 21. Mouse IgG_{2b} protein levels in mouse sera were measured using the Mouse IgG_{2b} ELISA Quantitation Set (Bethyl Laboratories, Inc., Montgomery, TX, USA) to estimate MM tumor burdens. Bone specimens were analyzed by X-ray and μCT images using SOFTEX OSM (SOFTEX Corporation, Kanagawa, Japan) and Latheta LCT-200 (Hitachi Aloka Medical, Tokyo, Japan), respectively. 2D images were reconstructed into 3D images with Amira software (Thermo Fischer Scientific).

Immunohistochemistry

After treatment, the tibiae were isolated and fixed for 2 days in 10% PFA/PBS, decalcified in 10% EDTA for 1 week at 4°C, and embedded in paraffin. Five μm-thick serial sections were prepared. After deparaffinization, the sections were incubated with anti-cathepsin K (Santa Cruz) overnight at 4°C. A horseradish peroxidase-streptavidin detection system (Dako, Carpinteria, CA) was used to detect the immunoreactivity.

Bone histomorphometry

For bone histomorphometry, mice were injected subcutaneously with 20 mg/kg tetracycline hydrochloride on Day 5 and 16 mg/kg calcein on Day 2 before sacrifice. All the right tibiae were fixed in 70% ethanol immediately after μCT analysis. The specimens were stained with Villanueva bone stain, embedded in methyl methacrylate without decalcification. The resulting blocks of the specimens were sectioned in the frontal plane at a thickness of 5 μm with a microtome (RM2255; Leica Biosystems, Nussloch, Germany). Bone histomorphometric analysis was performed using semiautomatic image analysis software (System Supply, Nagano,

Japan) and an optical fluorescence microscope. The following parameters were measured in the secondary spongiosa, extending 1.3–3.9 mm distally from the proximal growth cartilage of the tibia: bone volume/total volume (BV/TV, %); osteoid volume/total volume (OV/TV, %); osteoblast surface/bone surface (Ob.S/BS, %); osteoid surface/bone surface (OS/BS, %); trabecular thickness (Tb.Th, μm); osteoclast surface/bone surface (Oc.S/BS, %); eroded surface/bone surface (ES/BS, %); osteoclast number/bone surface (N.Oc/BS, mm^{-1}); mineralizing surface/bone surface (MS/BS, %); mineral apposition rate (MAR, μm/day); bone formation rate/bone volume (BFR/BV, %/year); and erosion depth (μm).

Ovariectomized mouse model and bone histomorphometric analysis

Female C57BL/6 mice were purchased from Japan SLC (Shizuoka, Japan). The mice at 4 months of age were subjected to ovariectomy (OVX) or to a sham operation (sham). The mice were divided into three groups with four mice each: sham-operated mice (Sham), OVX mice treated with saline (OVX) or with LLZ-1640-2 (LLZ) (OVX+LLZ). LLZ at 20 mg/kg or saline were intraperitoneally injected every other day for 4 weeks after the operation. After the treatment, the mice were sacrificed, and the lumbar vertebrae were collected and bone

morphological analysis was performed using a μCT SkyScan 1072 (SkyScan, Kartuizersweg, Belgium).

SUPPLEMENTARY FIGURE LEGENDS

Supplementary Figure 1. TAK1 inhibition does not impair the viability of normal PBMCs.

Normal human PBMCs were incubated in triplicate in the presence or absence of the TAK1 inhibitor LLZ1640-2 (LLZ) for 48 hours. LLZ was added at the indicated concentrations. Cell viability was measured using a WST-8 assay. Data are expressed as means ± SD.

Supplementary Figure 2. TAK1 inhibition abolishes CAM-DR to doxorubicin

Human BMSCs in 24-well culture plates were cultured overnight with or without LLZ1640-2 (LLZ) at 5 μM. Then, MM cell lines, RPMI8226 and MM.1S, were cultured alone or cocultured with the BMSCs for 24 hours in the presence or absence of doxorubicin (Dox) at 3 μM as indicated. After gentle pipetting, the MM cells were collected, and their viability was measured using a WST-8 assay.

Supplementary Figure 3. TAK1 inhibition suppresses integrin β1 expression in MM cells.

MM cell lines as indicated were treated for 24 hours with LLZ1640-2 (LLZ) at 5 μM. Cell lysates were collected, and the protein levels of integrin α_4 and integrin β_1 were analyzed using western

blotting. β-actin was used as a loading control.

Supplementary Figure 4. Fluorescent microscopic image of adhered MM cells.

Human BMSCs were treated with LLZ1640-2 (LLZ) at 5 μM for 1 day, and BCECF-AM-labeled MM cells were then added at 10^5 cells/well, and incubated for 4 hours. By gentle pipetting, non-adherent MM cells were removed, and adherent MM cells were observed using a fluorescence microscope. Green color indicates adhered MM cells. Representative images of three independent experiments are shown. Original magnification, ×20.

Supplementary Figure 5. TAK1 inhibition does not impair the viability of BMSCs.

BMSCs were incubated in triplicate in the presence or absence of the TAK1 inhibitor LLZ1640-2 (LLZ) for 48 hours. LLZ was added at the indicated concentrations. Cell viability was measured using a WST-8 assay. Data are expressed as means ± SD.

Supplementary Figure 6. TAK1 inhibition suppresses VEGF production by MM cells.

The indicated MM cell lines were cultured with or without LLZ1640-2 (LLZ) for 2 days (Upper).

The MM cell lines transduced with scrambled or TAK1 siRNA were cultured for 2 days (Lower). The concentrations of VEGF in their culture media were measured by ELISA. Data are shown as mean±SD. (n=4).

Supplementary Figure 7. TAK1 inhibition prevents ovariectomy (OVX)-induced bone loss. Four-month-old female C57/BL6 mice were sham-operated or ovariectomized. OVX mice were then treated with vehicle (saline) (OVX) or LLZ1640-2 at 20 mg/kg (OVX-LLZ) every other day by peritoneal injection for 4 weeks. μCT analysis was then performed to analyze changes in bone microstructure. Representative μCT images of the lumbar vertebral body from sham, OVX and OVX-LLZ groups are shown (upper). Parameters including the bone volume to the total volume (BV/TV), trabecular thickness (Tb.Th), trabecular numbers (Tb.N) and trabecular separation (Tb.Sp) were determined by μCT images using μCT SkyScan 1072 (lower).

SUPPLEMENTARY REFERENCES

1. Abe M, Hiura K, Wilde J, et al. Osteoclasts enhance myeloma cell growth and survival via cell-cell contact: a vicious cycle between bone destruction and myeloma expansion. Blood.

2004;104(8):2484-2491.

2. Abe M, Hiura K, Wilde J, et al. Role for macrophage inflammatory protein (MIP)-1alpha and MIP-1beta in the development of osteolytic lesions in multiple myeloma. Blood. 2002;100(6):2195-2202.

3. Kagawa K, Nakano A, Miki H, et al. Inhibition of TACE activity enhances the susceptibility of myeloma cells to TRAIL. PloS one. 2012;7(2):e31594.

4. Teramachi J, Morimoto H, Baba R, Doi Y, Hirashima K, Haneji T. Double stranded RNA-dependent protein kinase is involved in osteoclast differentiation of RAW264.7 cells in vitro. Exp Cell Res. 2010;316(19):3254-3262.

5. Teramachi J, Hiasa M, Oda A, et al. Pim-2 is a critical target for treatment of osteoclastogenesis enhanced in myeloma. Br J Haematol. 2018;180(4):581-585.

6. Tenshin H, Teramachi J, Oda A, et al. TAK1 inhibition subverts the osteoclastogenic action of TRAIL while potentiating its antimyeloma effects. Blood Adv. 2017;1(24):2124-2137.

7. Hiasa M, Teramachi J, Oda A, et al. Pim-2 kinase is an important target of treatment for tumor progression and bone loss in myeloma. Leukemia. 2015;29(1):207-217.

Supplementary Figure 1

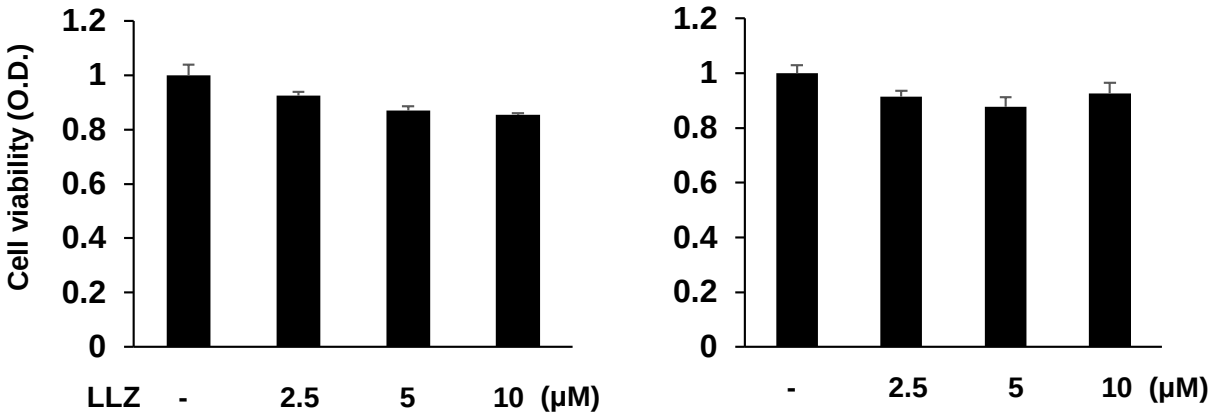

Supplementary Figure 2

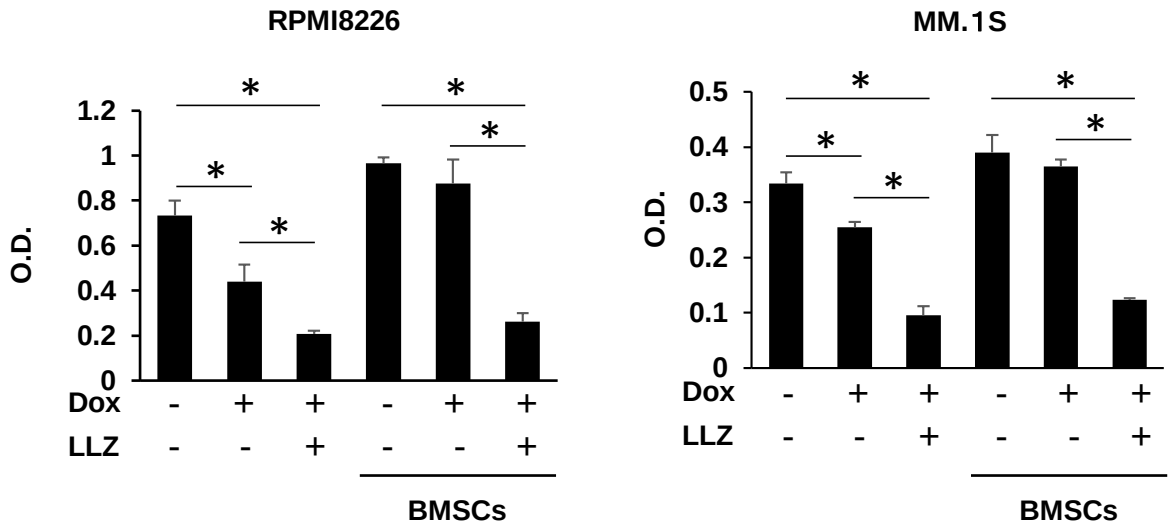

Supplementary Figure 3

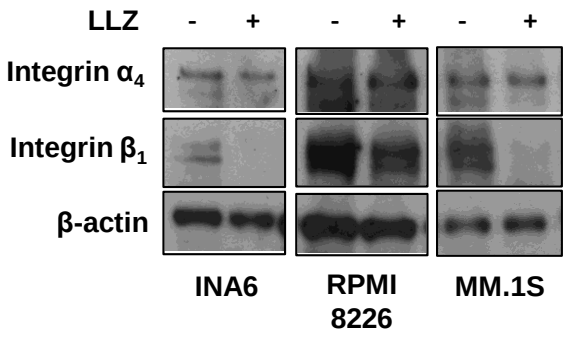

Supplementary Figure 4

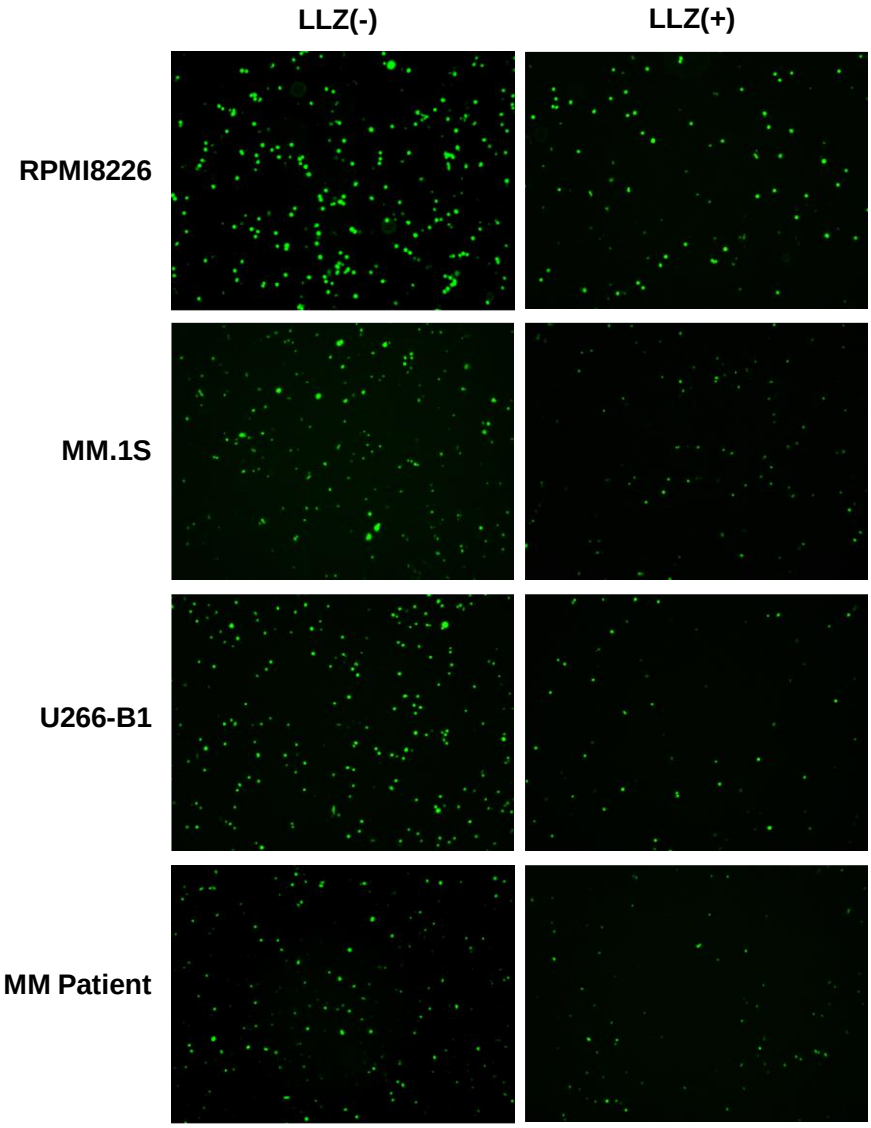

Supplementary Figure 5

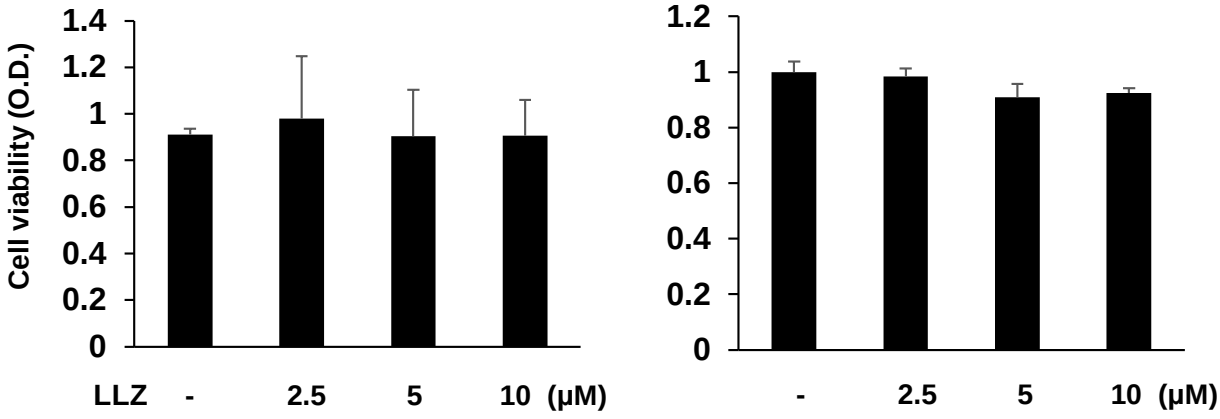

Supplementary Figure 6

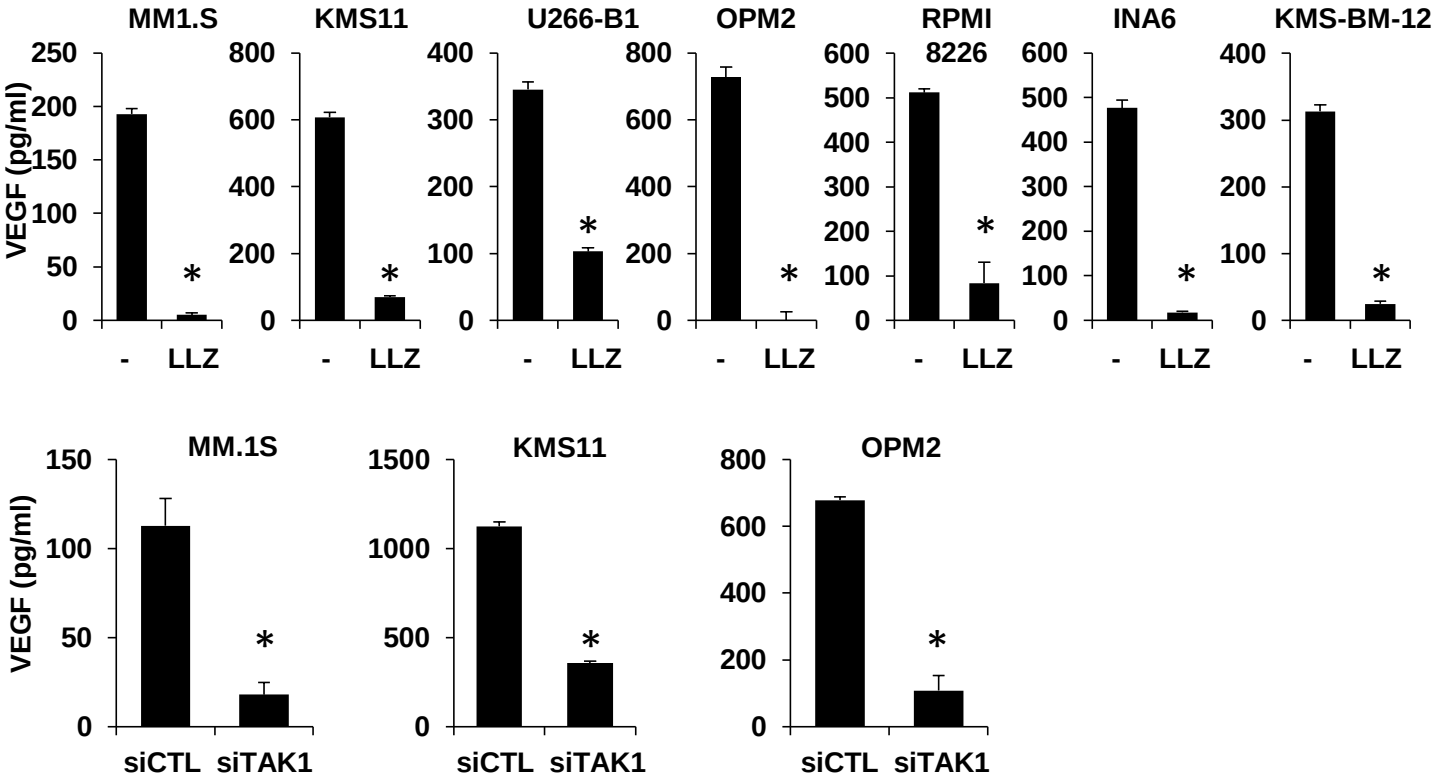

Supplementary Figure 7